

See discussions, stats, and author profiles for this publication at:
<https://www.researchgate.net/publication/229230102>

Matrix isolation infrared spectroscopic and density functional theoretical studies of the reactions of silver and gold atoms with carbon disulfide

ARTICLE *in* CHEMICAL PHYSICS · JULY 2003

Impact Factor: 1.65 · DOI: 10.1016/S0301-0104(03)00290-8

CITATIONS

6

READS

9

4 AUTHORS, INCLUDING:



Qingyu Kong

Argonne National Laboratory

65 PUBLICATIONS 1,123 CITATIONS

SEE PROFILE



Mingfei Zhou

Fudan University

260 PUBLICATIONS 5,085 CITATIONS

SEE PROFILE

Matrix isolation infrared spectroscopic and density functional theoretical studies of the reactions of silver and gold atoms with carbon disulfide

Aihua Zeng, Qingyu Kong, Yun Wang, Mingfei Zhou*

*Shanghai Key Laboratory of Molecular Catalysts and Innovative Materials,
Department of Chemistry, Fudan University, Shanghai 200433, PR China*

Received 24 April 2003; in final form 24 April 2003

Abstract

The reactions of silver and gold atoms with carbon disulfide in solid argon have been investigated with infrared absorption spectroscopy. The ground state silver and gold atoms reacted with carbon disulfide to form the sulfur-bonded $\text{Ag-}\eta^1\text{-SCS}$ and $\text{Au-}\eta^1\text{-SCS}$ complexes spontaneously on annealing. The $\text{Ag-}\eta^1\text{-SCS}$ and $\text{Au-}\eta^1\text{-SCS}$ complexes underwent photochemical rearrangement to the inserted SAgCS and SAuCS molecules upon ultraviolet–visible irradiation. The product molecules were identified based on isotopic IR spectra and density functional theory calculations.

© 2003 Published by Elsevier Science B.V.

1. Introduction

The chemistry of transition metal centers with various ligands has attracted considerable attention because of its catalytic and biological importance. The coordination chemistry of the CS_2 molecule with transition metal centers has been extensively studied [1–5]. CS_2 is generally very reactive toward transition metal centers: it forms numerous modes of coordination complexes with one or more transition metals and undergoes a

variety of insertion or disproportionation reactions [2–4].

The investigation of the interactions between transition metal atoms and CS_2 provides fundamental information about the reaction mechanism and the basic properties of binary transition metal complexes of CS_2 . Previous experimental and theoretical studies have provided a wealth of insight concerning the reactivity of transition metal atoms and ions with CS_2 molecules [6–14]. Guided ion beam mass spectrometric studies in the gas phase showed that the reactions of first-row transition metal cations with CS_2 to give MS^+ and MCS^+ . The results also suggest that the initial reaction step is predominantly insertion of the metal ion into the C–S bond to form the SM^+CS

* Corresponding author. Tel./fax: +86-21-65643532.
E-mail address: mfzhou@fudan.edu.cn (M. Zhou).

intermediate [6–9]. Matrix isolation spectroscopic studies showed that nickel atom reacted with CS_2 to form the $\text{Ni}(\text{CS}_2)_x$ complexes, with $x = 1\text{--}3$ [10]. Recently, the reactions of Co, Ni and Cu atoms with CS_2 in solid argon have been studied by Zhou and Andrews [11]. The carbon-bonded $\text{M}-\eta^1\text{-CS}_2$ and side-bonded $\text{M}-(\eta^2\text{-CS})\text{S}$ complexes were formed on annealing, whereas the inserted SMCS molecules were formed on photolysis. The mechanisms of the V and Cu + CS_2 reactions have also been theoretically investigated using density functional and coupled cluster calculations. The structures, spectra and relative stabilities for different possible complexes and the insertion product have been computed, and the possible routes for the formation of the insertion product on the potential energy surface have been discussed [12,13]. In this paper, we report a study of the reactions of Ag and Au atoms with CS_2 in solid argon. We will show that the sulfur-bonded $\text{M}-\eta^1\text{-SCS}$ complexes were formed, which were rearranged to the insertion SMCS molecules on photolysis.

2. Experimental and computational methods

The experimental setup for pulsed laser ablation and matrix infrared spectroscopic investigation has been described in detail previously [15,16]. Briefly, the 1064 nm fundamental of a Nd:YAG laser (10 Hz repetition rate and 8 ns pulse width) was focused onto the rotating silver or gold metal target through a hole in a CsI window. The laser-ablated metal atoms were codeposited with CS_2 in excess argon onto the 4 K CsI window for 1 h at a rate of 3–5 mmol/h. Infrared spectra were recorded on a Bruker Equinox 55 spectrometer at 0.5 cm^{-1} resolution using a DTGS detector. Matrix samples were annealed at different temperatures, and selected samples were subjected to broadband photolysis using a high pressure mercury arc lamp (25 W, without globe). CS_2/Ar samples were prepared in a stainless steel vacuum line using standard manometric technique. CS_2 was cooled to 77 K using liquid N_2 and evacuated to remove volatile impurities.

Quantum chemical calculations were performed to predict the structure and vibrational frequencies

of the potential reaction products using the Gaussian 98 program [17]. The three parameter hybrid functional according to Becke with additional correlation corrections to the Lee, Yang, and Parr (B3LYP) was utilized [18,19]. The 6-311+G* basis set for C and S atoms, and the Los Alamos ECP plus DZ (LANL2DZ) basis set for metal atoms were used for all calculations. The geometries were fully optimized and harmonic vibrational frequencies calculated with analytical second derivatives, and zero point vibrational energies (ZPVE) were derived.

3. Results and discussions

3.1. Infrared spectra

Experiments were done for laser-ablated silver and gold atom reactions with CS_2 in excess argon using laser energy ranging from 5 to 10 mJ/pulse with different CS_2 concentrations (0.1–0.5%). Typical infrared spectra in important frequency region are shown in Figs. 1 and 2, and the product absorptions are listed in Table 1. Different temperature annealing and broadband photolysis were done as demonstrated in Figs. 1 and 2 to characterize the absorption species.

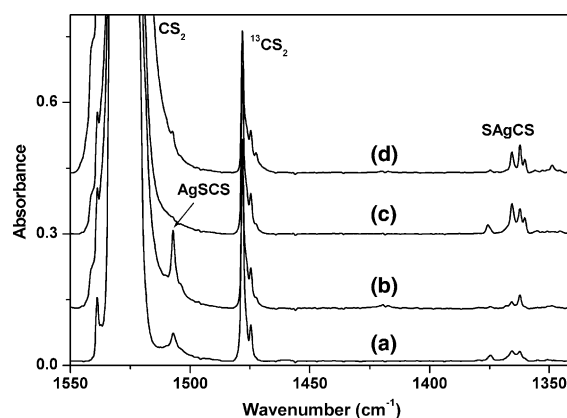


Fig. 1. Infrared spectra in the $1550\text{--}1340\text{ cm}^{-1}$ region from co-deposition of laser-ablated silver atoms with 0.5% CS_2 in argon. (a) One hour sample deposition at 4 K, (b) after annealing to 30 K, (c) after 20 min broadband photolysis, and (d) after annealing to 35 K.

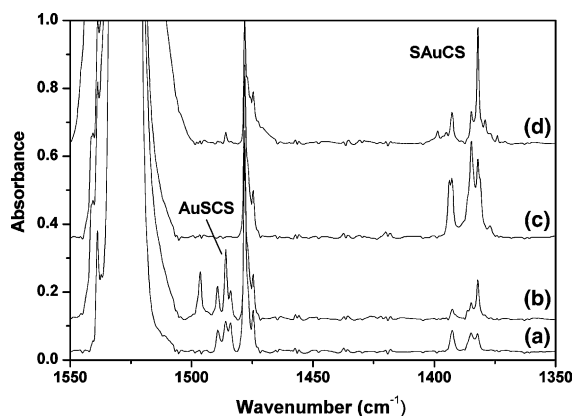


Fig. 2. Infrared spectra in the 1550–1350 cm^{-1} region from codeposition of laser-ablated gold atoms with 0.5% CS_2 in argon. (a) One hour sample deposition at 4 K, (b) after annealing to 30 K, (c) after 20 min broadband photolysis, and (d) after annealing to 35 K.

Experiments were repeated with $^{13}\text{CS}_2$ sample, and the isotopic frequencies are also listed in Table 1. Similar experiments with $^{12}\text{CS}_2 + ^{13}\text{CS}_2$ mixture were also done, and diagnostic spectra are shown in Figs. 3 and 4, respectively.

3.2. Calculation results

Five different possible geometric MCS_2 isomers were considered. Two minima, namely, the $\text{Ag-}\eta^1\text{-SCS}$ complex and the inserted SAgCS molecule have been located on the $\text{Ag} + \text{CS}_2$ potential energy surface. Four minima, namely, the $\text{Au-}\eta^1\text{-SCS}$, $\text{Au-}(\eta^2\text{-CS})\text{S}$ and $\text{Au-}\eta^1\text{-CS}_2$ complexes and the SAuCS insertion molecule have been located on the $\text{Au} + \text{CS}_2$ potential energy surface. The optimized equilibrium geometries are shown in Fig. 5. Table 2 shows the total energies and relative energies of the

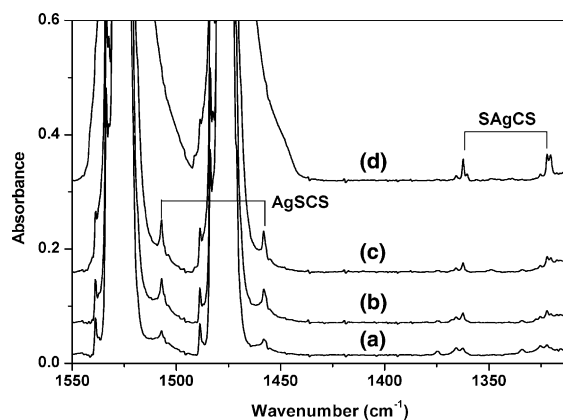


Fig. 3. Infrared spectra in the 1550–1310 cm^{-1} region from codeposition of laser-ablated silver atoms with 0.25% $^{12}\text{CS}_2 + 0.25\%$ $^{13}\text{CS}_2$ in argon. (a) One hour sample deposition at 4 K, (b) after annealing to 25 K, (c) after annealing to 30 K, and (d) after 20 min broadband photolysis.

different stationary points. The calculated harmonic vibrational frequencies and intensities are listed in Table 3. Both the $\text{Ag-}\eta^1\text{-SCS}$ complex and the inserted SAgCS molecule have doublet ground state. The $\text{Ag-}\eta^1\text{-SCS}$ complex is bound by 1.2 kcal/mol with respect to the ground state reactants. The insertion product lies 33.5 kcal/mol higher in energy than the $\text{Ag-}\eta^1\text{-SCS}$ complex. On the $\text{Au} + \text{CS}_2$ potential energy surface, the most stable isomer is the $\text{Au-}\eta^1\text{-SCS}$ complex, bound by 4.1 kcal/mol with respect to the reactants. The inserted SAuCS molecule is 11.9 kcal/mol higher in energy than the $\text{Au-}\eta^1\text{-SCS}$ complex.

3.3. $\text{Ag-}\eta^1\text{-SCS}$

As shown in Fig. 1, absorption at 1507.1 cm^{-1} in the $\text{Ag} + \text{CS}_2/\text{Ar}$ experiments appeared on sample

Table 1
Infrared absorptions (cm^{-1}) from codeposition of laser-ablated silver or gold atoms with CS_2 in excess argon

$^{12}\text{CS}_2$	$^{13}\text{CS}_2$	$^{12}\text{CS}_2 + ^{13}\text{CS}_2$	$R(12/13)$	Assignment
1507.1	1458.2	1507.1, 1458.2	1.03353	AgSCS
1365.6	1325.3	1365.6, 1325.3	1.03040	SAgCS site
1362.2	1322.0	1362.2, 1322.0	1.03041	SAgCS
1496.2	1448.0	1496.2, 1448.0	1.03329	AuSCS site
1485.9	1437.7	1485.9, 1437.7	1.03353	AuSCS
1392.6	1349.7	1392.6, 1349.7	1.03178	SAuCS site
1382.2	1339.6	1382.2, 1339.6	1.03180	SAuCS

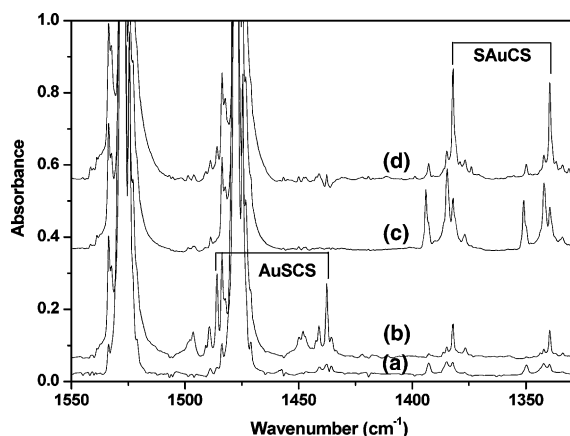


Fig. 4. Infrared spectra in the 1550–1330 cm^{-1} region from co-deposition of laser-ablated gold atoms with 0.25% $^{12}\text{CS}_2$ + 0.25% $^{13}\text{CS}_2$ in argon. (a) One hour sample deposition at 4 K, (b) after annealing to 30 K, (c) after 20 min broadband photolysis, and (d) after annealing to 35 K.

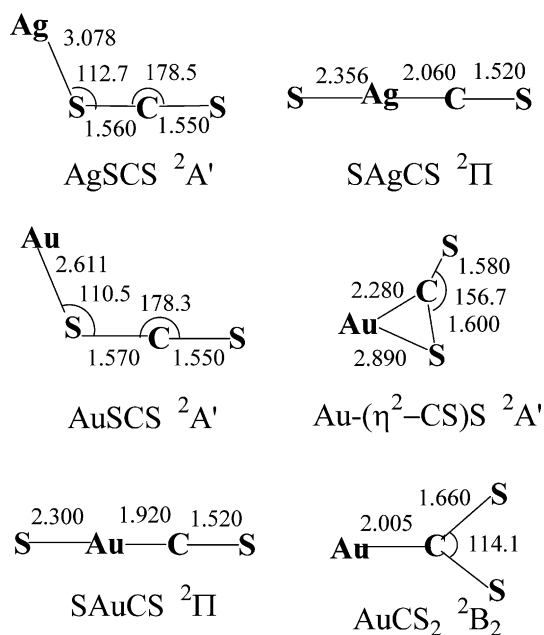


Fig. 5. Optimized structures of the MCS_2 ($\text{M} = \text{Ag}, \text{Au}$) isomers (bond length in Å, bond angle in degree).

deposition, increased markedly on annealing to 25 K, and was destroyed on broadband photolysis, when absorption at 1362.2 cm^{-1} due to SAgCS greatly increase. This band is only about 20.9 cm^{-1} lower than the antisymmetric stretching vibration

Table 2

Total energies (after zero point energy correction, in a.u.) and relative energies (kcal/mol) for the different stationary points calculated on the $\text{M} + \text{CS}_2$ ($\text{M} = \text{Ag}, \text{Au}$) potential energy surface

	Total energy	Relative energy
Ag	−145.75868	
CS_2	−834.54566	
$\text{Ag} + \text{CS}_2$	−980.30434	0
$\text{Au-}\eta^1\text{-SCS}$	−980.30630	−1.2
SAgCS	−980.25287	32.3
Au	−135.43978	
$\text{Au} + \text{CS}_2$	−969.98985	0
$\text{Au-}\eta^1\text{-SCS}$	−969.99194	−4.1
SAuCS	−969.97293	7.8
$\text{Au-}\eta^1\text{-CS}_2$	−969.96193	14.8
$\text{Au-}(\eta^2\text{-CS})\text{S}$	−969.97972	3.6

of the CS_2 molecule in solid argon. It shifted to 1457.8 cm^{-1} when $^{13}\text{CS}_2$ sample was used, and defined an isotopic $^{12}\text{C}/^{13}\text{C}$ ratio of 1.0338. This ratio is about the same as that of the antisymmetric stretching vibration of the CS_2 molecule. The band position and the isotopic frequency ratio suggest that the 1507.1 cm^{-1} band is due to an antisymmetric SCS stretching vibration of a CS_2 complex. In the mixed $^{12}\text{CS}_2 + ^{13}\text{CS}_2$ experiments, only the pure isotopic counterparts were observed, which indicates that only one CS_2 molecule is involved in this complex.

As has been mentioned, our DFT calculations predicted that the $\text{Ag-}\eta^1\text{-SCS}$ complex is the only stable complex form for AgCS_2 , which is 1.2 kcal/mol lower in energy than the separate reactants. The antisymmetric SCS stretching vibrational frequency was computed at 1537.7 cm^{-1} , which is in good agreement with the observed value. The calculated isotopic $^{12}\text{C}/^{13}\text{C}$ ratio of 1.0342 also fits the experimental value very well. This vibration was predicted to be the most intense mode for $\text{Ag-}\eta^1\text{-SCS}$, all the other modes were predicted to have very low IR intensities (Table 3).

3.4. $\text{Au-}\eta^1\text{-SCS}$

Similar absorption at 1485.9 cm^{-1} in the $\text{Au} + \text{CS}_2/\text{Ar}$ experiments is assigned to the $\text{Au-}\eta^1\text{-SCS}$ complex. This band is weak on sample deposition, increased greatly on annealing, and disappeared on broadband photolysis (Fig. 2). It shifted to

Table 3

Calculated vibrational frequencies (cm^{-1}) and intensities (km/mol) for the $\text{Ag-}\eta^1\text{-SCS}$, SAgCS , $\text{Au-}\eta^1\text{-SCS}$, SAuCS , $\text{Au-}\eta^1\text{-CS}_2$ and $\text{Au-}(\eta^2\text{-CS})\text{S}$ molecules

	Frequency (intensity)			
$\text{Ag-}\eta^1\text{-SCS}$	1537.7(806)	663.7(7)	394.2(1)	381.8(37)
	64.6(0)	29.0(0)		
SAgCS	1373.4(637)	331.0(10)	257.8(2)	235.5(5)
	235.4(13)	44.2(1)	42.8(1)	
$\text{Au-}\eta^1\text{-SCS}$	1519.9(764)	653.9(5)	386.5(1)	370.6(37)
	129.5(0.5)	51.0(0)		
$\text{Au-}(\eta^2\text{-CS})\text{S}$	1336.0(410)	614.6(63)	398.5(5)	260.5(132)
	60.3(7)	49.8(33)		
$\text{Au-}\eta^1\text{-CS}_2$	922.6(248)	908.6(3)	396.1(14)	367.0(9)
	195.9(4)	159.6(8)		
SAuCS	1407.6(652)	363.5(0)	354.2(8)	338.0(14)
	333.4(2)	59.5(0)	59.1(0)	

1437.7 cm^{-1} with $^{13}\text{CS}_2$. The isotopic $^{12}\text{C}/^{13}\text{C}$ ratio (1.0335) indicates that this band is due to an anti-symmetric SCS stretching vibration. The doublet isotopic structure in the mixed $^{12}\text{CS}_2 + ^{13}\text{CS}_2$ spectra shows that only one CS_2 is involved in this mode. The assignment is supported by DFT calculations, which found a stable $\text{Au-}\eta^1\text{-SCS}$ complex with strong stretching vibration at 1519.9 cm^{-1} .

The above assigned $\text{Ag-}\eta^1\text{-SCS}$ and $\text{Au-}\eta^1\text{-SCS}$ complexes both have $^2\text{A}'$ ground state with bent structure, which correlate to the ground state metal atoms and CS_2 . The bonding in these complexes is quite similar to that of the carbonyl complexes, which has been the subject of considerable studies [20]. As the d_σ shell of metal is partially filled, the CS_2 to metal σ donation is small, and the metal–SCS bonding is weak. The binding energies of $\text{Ag-}\eta^1\text{-SCS}$ and $\text{Au-}\eta^1\text{-SCS}$ were predicted to be only 1.2 and 4.1 kcal/mol, respectively, with respect to the ground state reactants. We note that AgCO is unbound with respect to ground state Ag atom and CO, whereas CuCO and AuCO are weakly bounded complexes [20]. The $\text{Ag-}\eta^1\text{-SCS}$ and $\text{Au-}\eta^1\text{-SCS}$ complexes prefer bent geometry to reduce the repulsion between the metal s and the SCS σ orbitals analogous to the CuCO and CuCS molecules [21–23].

3.5. SAgCS

The band at 1362.2 cm^{-1} is weak after sample deposition, sharpened on annealing, but markedly

increased on broadband photolysis (Fig. 1). The increase upon photodestruction of $\text{Ag-}\eta^1\text{-SCS}$ implies that the new product is generated from $\text{Ag-}\eta^1\text{-SCS}$. The 1362.2 cm^{-1} band shifted to 1322.0 cm^{-1} with $^{13}\text{CS}_2$, giving an isotopic $^{12}\text{C}/^{13}\text{C}$ ratio of 1.0304. This ratio is quite different from that of the $\text{Ag-}\eta^1\text{-SCS}$ complex, and is likely due to the CS stretching vibration of a thiocarbonyl species. In the mixed $^{12}\text{CS}_2 + ^{13}\text{CS}_2$ spectra, only pure isotopic counterparts were produced, which indicates that only one CS subunit is involved in this vibration. Therefore, we assign the 1362.2 cm^{-1} band to the CS stretching vibration of the SAgCS molecule. Similar insertion products have been observed in previous metal + CS_2 reactions [11].

The assignment was further supported by DFT calculations, which predicted that the inserted SAgCS molecule has a doublet ground state with a linear structure. The CS stretching vibration was predicted at 1373.4 cm^{-1} for SAg^{12}CS and 1330.5 cm^{-1} for SAg^{13}CS , which are in good agreement with the experimental values. The calculation indicates that the CS stretching vibration has the largest IR intensity (637 km/mol , versus less than 13 km/mol for the other vibrational modes).

3.6. SAuCS

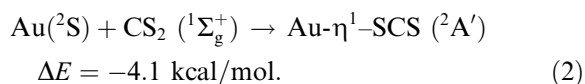
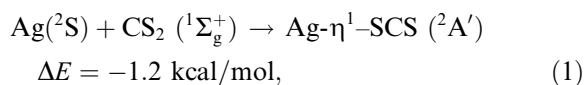
Similar absorption at 1382.2 cm^{-1} in the $\text{Au} + \text{CS}_2$ experiments is assigned to the SAuCS molecule following the example of SAgCS . The 1382.2 cm^{-1} band increased greatly upon broad-

band photolysis with simultaneous disappearance of the $\text{Au-}\eta^1\text{-SCS}$ complex. It shifted to 1339.6 cm^{-1} with $^{13}\text{CS}_2$. The $^{12}\text{C}/^{13}\text{C}$ ratio of 1.0318 implies that this band is a CS stretching vibration. The mixed $^{12}\text{CS}_2 + ^{13}\text{CS}_2$ spectra shown in Fig. 4 confirmed that only one CS is involved in this mode. Density functional calculations predicted a linear doublet ground state molecule with strong CS stretching vibration at 1407.6 cm^{-1} (652 km/mol) with isotopic $^{12}\text{C}/^{13}\text{C}$ ratio of 1.0322. The vibrational frequencies of other modes are lower than 400 cm^{-1} with very low intensities (Table 3).

The inserted SAgCS and SAuCS molecules can be viewed as the interaction of AgS (AuS) and CS. The AgS (AuS) molecule has a $^2\pi$ ground state. The interactions between AgS (AuS) and CS are dominated by donations from the filled σ orbital of CS into acceptor orbital on AgS (AuS) and backdonations from the filled π orbitals of AgS (AuS) to the antibonding π^* orbitals of CS. The binding energies of SAgCS and SAuCS were computed to be 26.6 and 45.9 kcal/mol with respect to $\text{AgS} + \text{CS}$ and $\text{AuS} + \text{CS}$.

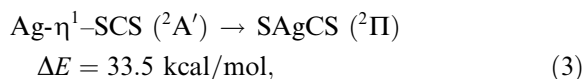
3.7. Reaction mechanism

The spectra in Figs. 1 and 2 clearly demonstrate that ground state silver and gold atoms react with carbon disulfide in solid argon to form the $\text{Ag-}\eta^1\text{-SCS}$ and $\text{Au-}\eta^1\text{-SCS}$ complexes. The absorptions of these complexes increased markedly upon annealing indicating that reactions (1) and (2) require negligible activation energy



The coordination of CS_2 to the first row transition metal atoms is different from that of Ag and Au. In the reactions of Co, Ni and Cu atoms with CS_2 in solid argon, the $\text{M-}\eta^1\text{-SCS}$ complexes were not formed, whereas the carbon-bonded $\text{M-}\eta^1\text{-CS}_2$ and side-bonded $\text{M-}(\eta^2\text{-CS})\text{S}$ complexes were observed [11].

The absorptions due to the inserted SAgCS and SAuCS molecules increased on broadband photolysis, during which the absorptions of the $\text{Ag-}\eta^1\text{-SCS}$ and $\text{Au-}\eta^1\text{-SCS}$ complexes disappeared. These observations suggest that $\text{Ag-}\eta^1\text{-SCS}$ and $\text{Au-}\eta^1\text{-SCS}$ underwent photoinduced isomerism to the inserted SAgCS and SAuCS molecules, as shown in reactions (3) and (4)



These isomerization reactions were predicted to be endothermic. The inserted molecules were only observed on broadband photolysis, which suggests that reactions (3) and (4) require activation energy. Recent theoretical study on the $\text{Cu} + \text{CS}_2$ reaction showed that the formation of the insertion product needs to overcome an energy barrier of at least 26 kcal/mol with respect to the ground state reactants [13].

4. Conclusions

The reactions of silver and gold atoms with carbon disulfide in solid argon have been investigated by a combination of matrix isolation infrared absorption spectroscopy and density functional theoretical calculations. Our results indicate that the ground state silver and gold atoms reacted with carbon disulfide to form the sulfur-bonded $\text{Ag-}\eta^1\text{-SCS}$ and $\text{Au-}\eta^1\text{-SCS}$ complexes spontaneously in solid argon matrix on annealing. These complexes have doublet ground state with bent structure, and are weakly bound with respect to the ground state metal atoms and CS_2 . The $\text{Ag-}\eta^1\text{-SCS}$ and $\text{Au-}\eta^1\text{-SCS}$ complexes underwent photochemical rearrangement to the inserted SAgCS and SAuCS molecules upon ultraviolet–visible irradiation. These insertion products were predicted to have doublet ground state with linear structure. The aforementioned product molecules were identified based on isotopic IR spectra and density functional frequency calculations.

Acknowledgements

We greatly acknowledge financial support from NSFC (20003003 and 20125033) and the NKB-RSF of China.

References

- [1] M.C. Baird, G. Wilkinson, *Chem. Commun.* (1966) 267.
- [2] J.A. Ibers, *Chem. Soc. Rev.* 11 (1982) 57.
- [3] I.S. Butler, A.E. Fenster, *J. Organomet. Chem.* 66 (1974) 161.
- [4] P.V. Yaneff, *Coord. Chem. Rev.* 140 (1995) 37.
- [5] P.V. Broadhurst, N.E. Leadbeater, J. Lewis, P.R. Raithby, *J. Chem. Soc. Dalton Trans.* (1997) 4579.
- [6] C. Rue, P.B. Armentrout, I. Kretzschmar, D. Schroder, H. Schwarz, *J. Phys. Chem. A* 106 (2002) 9788.
- [7] C. Rue, P.B. Armentrout, I. Kretzschmar, D. Schroder, H. Schwarz, *Int. J. Mass Spectrom.* 210 (2001) 283.
- [8] C. Rue, P.B. Armentrout, I. Kretzschmar, D. Schroder, H. Schwarz, *J. Phys. Chem. A* 105 (2001) 8456.
- [9] C. Rue, P.B. Armentrout, I. Kretzschmar, D. Schroder, J.N. Harvey, H. Schwarz, *J. Chem. Phys.* 110 (1999) 7858.
- [10] H. Huber, G.A. Ozin, W.J. Power, *Inorg. Chem.* 16 (1977) 2234.
- [11] M.F. Zhou, L. Andrews, *J. Phys. Chem. A* 104 (2000) 4394.
- [12] I. Papai, Y. Hannachi, S. Gwizdala, J. Mascetti, *J. Phys. Chem. A* 106 (2002) 4181.
- [13] Y. Dobrogorskaya, J. Mascetti, I. Papai, A. Nemukhin, Y. Hannachi, *J. Phys. Chem. A* 107 (2003) 2711.
- [14] G.H. Jeung, *Chem. Phys. Lett.* 237 (1995) 65.
- [15] M.H. Chen, X.F. Wang, L.N. Zhang, M. Yu, Q.Z. Qin, *Chem. Phys.* 242 (1999) 81.
- [16] Q.Y. Kong, M.H. Chen, J. Dong, Z.H. Li, K.N. Fan, M.F. Zhou, *J. Phys. Chem. A* 106 (2002) 11709.
- [17] M.J. Frisch, G.W. Trucks, H.B. Schlegel, G.E. Scuseria, M.A. Robb, J.R. Cheeseman, V.G. Zakrzewski, J.A. Montgomery Jr., R.E. Stratmann, J.C. Burant, S. Dapprich, J.M. Millam, A.D. Daniels, K.N. Kudin, M.C. Strain, O. Farkas, J. Tomasi, V. Barone, M. Cossi, R. Cammi, B. Mennucci, C. Pomelli, C. Adamo, S. Clifford, J. Ochterski, G.A. Petersson, P.Y. Ayala, Q. Cui, K. Morokuma, D.K. Malick, A.D. Rabuck, K. Raghavachari, J.B. Foresman, J. Cioslowski, J.V. Ortiz, A.G. Baboul, B.B. Stefanov, G. Liu, A. Liashenko, P. Piskorz, I. Komaromi, R. Gomperts, R.L. Martin, D.J. Fox, T. Keith, M.A. Al-Laham, C.Y. Peng, A. Nanayakkara, C. Gonzalez, M. Challacombe, P.M.W. Gill, B. Johnson, W. Chen, M.W. Wong, J.L. Andres, C. Gonzalez, M. Head-Gordon, E.S. Replogle, J.A. Pople, *Gaussian 98, Revision A.7*, Gaussian, Pittsburgh, PA, 1998.
- [18] C. Lee, E. Yang, R.G. Parr, *Phys. Rev. B* 37 (1988) 785.
- [19] A.D. Becke, *J. Chem. Phys.* 98 (1993) 5648.
- [20] M.F. Zhou, L. Andrews, C.W. Bauschlicher Jr., *Chem. Rev.* 101 (2001) 1931, and references therein.
- [21] R. Fournier, *J. Chem. Phys.* 99 (1993) 1801.
- [22] C.W. Bauschlicher Jr., *J. Chem. Phys.* 100 (1994) 1215.
- [23] Q.Y. Kong, A.H. Zeng, M.H. Chen, M.F. Zhou, Q. Xu, *J. Chem. Phys.* 118 (2003) 7267.